



Pushing the boundaries  
of chemistry?  
It takes  
#HumanChemistry

Make your curiosity and talent as a chemist matter to the world with a specialty chemicals leader. Together, we combine cutting-edge science with engineering expertise to create solutions that answer real-world problems. Find out how our approach to technology creates more opportunities for growth, and see what chemistry can do for you at:

[evonik.com/career](https://www.evonik.com/career)



# Electrothermal Tristability Causes Sudden Burn-In Phenomena in Organic LEDs

Anton Kirch, Axel Fischer,\* Matthias Liero, Jürgen Fuhrmann, Annegret Glitzky, and Sebastian Reineke

Organic light-emitting diodes (OLEDs) have been established as a mature display pixel technology. While introducing the same technology in a large-area form factor to general lighting and signage applications, some key questions remain unanswered. Under high-brightness conditions, OLED panels were reported to exhibit nonlinear electrothermal behavior causing lateral brightness inhomogeneities and even regions of switched-back luminance. Also, the physical understanding of sudden device failure and burn-ins is still rudimentary. A safe and stable operation of lighting tiles, therefore, requires an in-depth understanding of these physical phenomena. Here, it is shown that the electrothermal treatment of thin-film devices allows grasping the underlying physics. Configurations of OLEDs with different lateral dimensions are studied as a role model and it is reported that devices exceeding a certain panel size develop three stable, self heating-induced operating branches. Switching between them causes the sudden formation of dark spots in devices without any preexisting inhomogeneities. A current-stabilized operation mode is commonly used in the lighting industry, as it ensures degradation-induced voltage adjustments. Here, it is demonstrated that a tristable operation always leads to destructive switching, independent of applying constant currents or voltages. With this new understanding of the effects at high operation brightness, it will be possible to adjust driving schemes accordingly, design more resilient system integrations, and develop additional failure mitigation strategies.

## 1. Introduction

Organic light-emitting devices (OLEDs) have become a standard technology for display applications<sup>[1–3]</sup> and are introduced to the lighting mass market.<sup>[4–6]</sup> They have been studied for decades and are well-understood devices. It is all the more surprising that we now found a Joule heating-induced tristable operation behavior that is unique to large-area devices. As yet, tristability was discussed for inorganic resonant tunneling diodes<sup>[7–9]</sup> and optically-pumped systems<sup>[10–12]</sup> but never for any kinds of thin-film lighting devices. It provides a profound understanding of electrothermal effects and sudden device failure connected to operation scenarios of thin-film lighting tiles at high brightness.


Elevated driving currents ( $>100 \text{ mA cm}^{-2}$ ) were shown to cause electrothermal feedback and non-linear device behavior,<sup>[13,14]</sup> resulting in lateral brightness and temperature inhomogeneities.<sup>[15–20]</sup> Only recently, electrothermal treatment was demonstrated to successfully describe these high-current phenomena in organic devices.<sup>[21–23]</sup> Modeling the current density versus voltage ( $JV$ ) characteristics of small

OLED pixels revealed that Joule self-heating induces a region of negative differential resistance (NDR).<sup>[24,25]</sup> In this region, an increase in driving current causes a reduction in voltage across the LED. Therefore, it produces two stable branches of positive differential resistance (PDR), a phenomenon called bistability. This study, now, indicates that the shape of the S-curve of the  $JV$  profile depends on the active device area. In large-area panels, the S-curvature is so pronounced that even three stable operating regimes occur, an effect called tristability and entailing severe implications to the device performance.

Sudden dark spot formation and device failure is an issue commonly observed for lighting devices and is compromising their reliability. Its origins, however, yet remained uncertain. Following typical expectations, manufacturing residuals and defects were suspected to trigger dark spot formation as degradation seeds.<sup>[4,26–31]</sup> Here, we show by contrast that an inherent electrothermal tristability triggers dark spot formation even for perfectly homogeneously fabricated devices. Using a 3D model, we can exactly pinpoint where and at which conditions branch

A. Kirch, A. Fischer, S. Reineke  
Dresden Integrated Center for Applied Physics and Photonic Materials (IAPP) and Institute of Applied Physics  
Technische Universität Dresden  
Nöthnitzer Straße 61, 01187 Dresden, Germany  
E-mail: axel\_fischer@tu-dresden.de

M. Liero, J. Fuhrmann, A. Glitzky  
Weierstrass Institute Berlin (WIAS)  
Mohrenstraße 39, 10117 Berlin, Germany

 The ORCID identification number(s) for the author(s) of this article can be found under <https://doi.org/10.1002/adfm.202106716>.

© 2021 The Authors. Advanced Functional Materials published by Wiley-VCH GmbH. This is an open access article under the terms of the Creative Commons Attribution-NonCommercial License, which permits use, distribution and reproduction in any medium, provided the original work is properly cited and is not used for commercial purposes.

DOI: 10.1002/adfm.202106716

transitions and the respective device failure will occur. As a result of tristability, a large-area OLED is prone to switching phenomena that cannot even be prevented by current-stabilized operation, as widely applied.<sup>[13,32,33]</sup>

## 2. Results

### 2.1. Electrothermal Simulations

In former studies, we used a 3D numerical simulation to self-consistently predict solutions for local heat dissipation and current density profiles in semiconductor devices. The model combines the continuity equation for the total current and heat. It is solved using a Voronoi box scheme that is adapted to our LED layer stack. Details on the code are provided by the maintaining team at WIAS and can be found in refs. [34, 35]. It successfully reproduces the entire *JV* curve of the investigated OLEDs (see Section S2, Supporting Information) until their degradation and has been applied recently to predict the Joule heating-induced Switch-back effect (SB), which explains the anomaly of distinct OLED regions becoming darker at increasing driving current.<sup>[23]</sup> Using this tool, we started investigating the relation between OLED panel size and the significance of electrothermal switching. We found an earlier emergence of the SB effect with increasing OLED panel size.<sup>[36]</sup> The ratio between lateral and vertical panel dimensions (centimeter versus hundreds of nanometer, respectively), setting the frame for electrical and thermal (de)coupling, is hence a key parameter for electrothermal influences on the device performance.

In this study, we discuss the general shape of the *JV* curve, which we found changing dramatically with panel size. Here, mean current density refers to the applied driving current divided by the active area and sensing voltage is the voltage

drop across the sensing electrodes, as specified in the subsequent section. **Figure 1A** depicts the simulated findings for quadratic OLEDs: the dashed line indicates an isothermal *JV* curve, where self-heating plays no role. Here, the panel size makes no difference. This operation scenario is only valid for devices that are run for a very short time, for example, at pulsed operation mode.<sup>[25,37]</sup> Any lighting or signage application (typically >1000 cd m<sup>-2</sup>), however, passes into electrothermal equilibrium over time, represented by the solid lines in **Figure 1A**. Whereas smaller devices show the well-known S-bend including one NDR region and two stable PDR operating branches (bistability), the simulation predicts the devices exceeding a size of (5mm)<sup>2</sup> to bend into an additional regime of PDR (**Figure 1B**, PDR 2). The equilibrium operating point of the device depends on the OLED panel size as well as the driving current. Considering a tristable operating curve, even little adaptations in current may have a tremendous impact on the operating point the LED finally reaches.

### 2.2. Access to Region PDR 2

Tristability can be understood as the combination of two overlapping bistabilities: one regarding voltages and one regarding currents. Now, neither current nor voltage can unambiguously identify the operating point of the LED. The switching along voltages is related to the bistability that is caused by the already known strong thermal activation of the electrical conductivity.<sup>[37]</sup> The switching along constant currents, however, is a new effect that is inherent to tristable behavior. It is only present if the devices exceed a certain area (cf., **Figure 1A**), which is why it is clear that no intrinsic device or material property causes this effect. It is rather related to the device geometry and the implied electric and thermal coupling within. As shown in **Figure 1C**, during switching along constant mean current

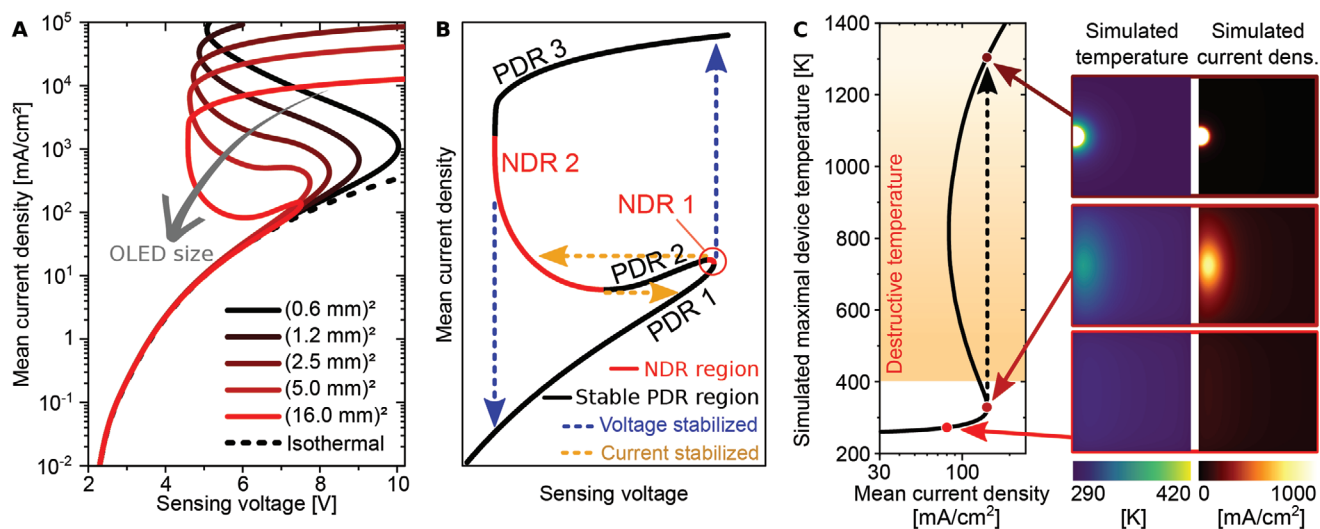


**Figure 1.** 3D PDE model results. A) Structural change of *JV* curves with varying OLED size. B) Close-up on the 16mm × 16mm device presenting three stable ( $dj/dV > 0$ ) operation regions and feasible transition paths. C) Simulated maximum temperature over mean current density of the 16 mm × 16 mm device. The inset shows the top-view temperature and current density distribution of the LED in the first stable region (light red), right before (dark red,  $T_{\max} = 360$  K) and right after the branch transition (brown,  $T_{\max} = 1300$  K). Please see Movie S1, Supporting Information for the full range of simulated temperature and current distributions and Section S3, Supporting Information for details on temperature stability.

densities, the current distribution reconfigures abruptly (see Movie S1, Supporting Information for the full range of simulated temperature and current distributions). For large-area devices there are up to three configurations of current and temperature distribution, respectively, that consume the very same total device driving current. Therefore, switching along constant mean current densities means that the OLED changes to a more attractive current distribution, for example, if there is no more solution in the branches NDR 1 or NDR 2.

Figure 1B schematically zooms into the  $16\text{mm} \times 16\text{mm}$  sample and shows how the different stable and unstable regions of the  $JV$  curve can be accessed: a voltage-stabilized measurement runs through the entire PDR 1 region and then jumps vertically into region PDR 3. Running the same scan backward provides access to the entire region PDR 3 and then jumps vertically into branch PDR 1 (blue arrows). So, neither a single NDR nor the PDR 2 region would be accessible. A current-stabilized scan, on the other hand, reaches the NDR 1 region (indicated in red) before jumping onto the PDR 3 branch. On its way back, the same scan enters the NDR 2 region and then jumps back onto the PDR 1 branch (yellow arrows). Again, region PDR 2 remains unengaged.

Reproducible branch-hopping experiments were demonstrated for a bistable n-i-n device, using  $C_{60}$  as intrinsic layer.<sup>[37]</sup> Reversible branch-hopping demonstrations for operating OLEDs, however, are extremely challenging due to their limited temperature stability and ongoing gradual degradation. Each branch transition, whether along the blue or orange path, occurs on very short time scales and coincides with an abrupt rearrangement of the current and heat distribution in the device region, as shown in Figure 1C. Hence, distinct device areas experience a sudden increase in temperature, electrical conductivity, and current that causes immediate local destruction and consequently the formation of dark spots. As a result of those regions consuming a vast share of the driving current just before burning-in, the remaining device areas are switched-back in current and temperature for a short period of time. Every attempt to operate an OLED at those interesting conditions, that is, right before jumping into another operating branch, is thus a destructive, single-shot measurement requiring a fresh device.

So far, it was expected that electrothermal feedback can be stabilized under constant-current mode. If the simulations describe the true behavior of the devices, however, also at constant current an electrothermal switching phenomenon can occur that leads to the destruction of the device.

With the previous considerations being made, the PDR 2 region can neither be accessed by current- nor by voltage-stabilized measurements. Yet, it appears feasible to detect switching events under constant-current operation that are caused by the transition from branch PDR 1 to PDR 3. Even if the device is damaged by the switching process, this effect should be experimentally accessible.

### 2.3. Experimental $JV$ Scan

In this section, we experimentally prove switching events by gradually increasing the mean driving current density. According to Figure 1A, a medium-sized OLED device exceeding

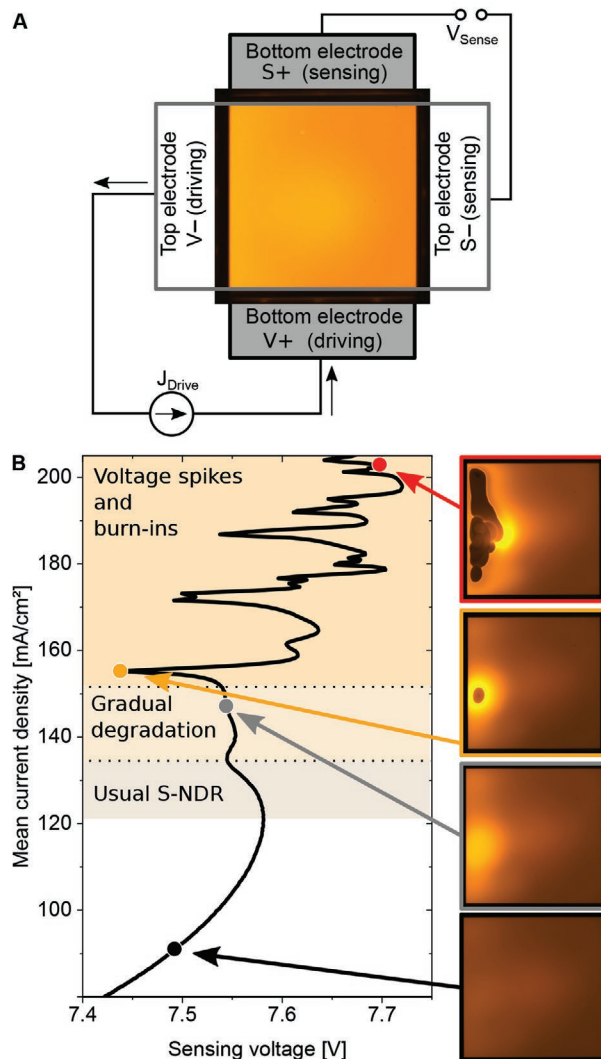


**Figure 2.** Experimental  $JV$  scan results. A) Device geometry to realize four-wire measurements. B) Current-stabilized  $JV$  scan and top-view images at distinct points of interest. Please see Movie S2, Supporting Information for the full range of measured data.

$5\text{mm} \times 5\text{mm}$  is large enough to show tristable behavior. For the following experiments, we fabricated devices with an active area of  $16\text{mm} \times 16\text{mm}$ . They are standard phosphorescent, red top-emitting devices as detailed in the Experimental Section. For  $JV$  characterization, we use a four-wire crossbar structure with two driving and two sensing contacts (cf., Figure 2A). In our setup geometry, the electron current injected at the top contact is coming from the left. The top electrode's sheet resistance is measured to be  $15\ \Omega/\square$ . Hence, the OLED is expected to become brighter on its left side. The device is embedded into a Peltier element-based cryostat under vacuum ( $<1\text{mbar}$ ) with a camera recording pictures from above, as detailed in ref. [23].

Figure 2B presents a current-stabilized  $JV$  scan with current steps of 1 mA. A top-view picture and the sensing voltage were taken after 2 s of stabilization at each step. The experimental curve shows three main domains after leaving the PDR 1 region:

First, the well-known S-shape due to Joule self-heating, representing an NDR region, is detected. Second, a domain develops where gradual degradation becomes severe and outcompetes the pure theoretical  $JV$  profile. This we ascribe to intrinsic transport and emission layer degradation, which reduces the electrical conductivity as expected for OLEDs at elevated thermal stress.<sup>[4]</sup> The sample, however, shows no sudden dark spot formation throughout this region and remains intact. Third, a domain of unprecedented voltage spikes, each of which coincides with burning-in of a dark spot into the active device area, is detected. This region cannot be explained by classical degradation mechanisms. Please see Movie S2, Supporting Information for the full range of measured data.

In fact, the experiment verifies the simulation-based expectation that the LED attempts a branch transition from PDR 1 to PDR 3 according to Figure 1B. This transition, however, is overlaid on the fly by a dramatic rise in local device temperature, which destroys it locally, confer, Figure 1C. The first dark spot appears where the simulation predicts the local temperature and current density to skyrocket and thus follows our model. In the further course of the driving current ramp-up, one can observe more and more of these scenarios, each coinciding with the burn-in of a dark spot. The spots, interestingly, arrange themselves symmetrically in the left center of the panel, where current and heat are at their maximum. As the remaining OLED area remains bright, such dark spots cannot be shorts. They are rather to be understood as regions of elevated electrical resistance.

#### 2.4. Switch-Back Effect and Tristability

This section focuses on the first burn-in incident of the device, as our simulation does not model the characteristics of a degraded sample. Therefore, we change the experimental settings to enable the deliberate steering of a device into the interesting regions of expected branch transitions. Now, the driving current is set manually and the sensing voltage is continuously monitored over time. The following discussion, therefore, uses

current versus voltage ( $IV$ ) characteristics. Figure 3A shows the applied driving current and Figure 3B the measured sensing voltage drop across the device.

For the presented period of time, the device operates already in its NDR 1 region (increasing driving current and decreasing sensing voltage). Each adjustment of the driving current is followed by a spike in voltage. The source measure unit (SMU) applies a higher voltage to achieve a higher current and the OLED subsequently passes into a new stable and self-consistent solution of current, voltage, and temperature distribution. There, it requires less applied voltage for the same current and thus the voltage profile shows a falling exponential function until stable operation. This decrease is overlaid with a gradual voltage increase due to ongoing intrinsic gradual degradation. After  $t = 175$  s something unprecedented and interesting happens: The OLED does not stabilize any longer but shows an abrupt drop in voltage, indicating that it becomes suddenly highly conductive, that is, that the temperature and thus current density are skyrocketing in a certain region of the device. This tiny area can be identified in picture (b), where suddenly a very bright spot arises. Please find the numerical brightness profiles of these pictures, demonstrating a spike in detected brightness, in the Section 7, Supporting Information. The voltage spike coincides with a sudden dark spot that is formed next to the driving electrode.

Figure 3C shows a series of images taken at certain operating points indicated in the voltage diagram. The first row presents the original camera picture. Note that they appear very dark, as we tried not to run the camera into saturation and hence drastically limited the exposure time. The second row gives the same picture in a different color coding. The term brightness refers to the pixel values in arbitrary units produced by the camera, as it does not measure luminance units. Brightness and luminance are proportional. The last row, finally, presents the change in brightness respective to picture (a). This is done by subtracting picture (a) from pictures (b), (c), and (d). Blue indicates a decreasing and red an increasing brightness. As can be seen from picture (b-a), the largest part of the OLED pixel is switched back in brightness and a significant share of current

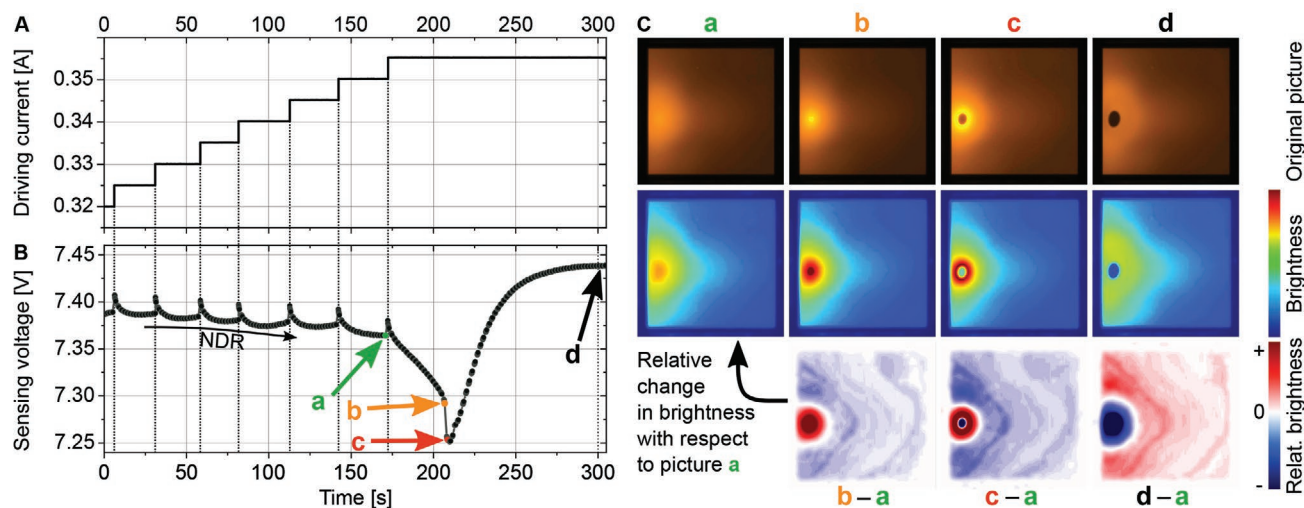


**Figure 3.** Dark spot formation is heralded by switched-back regions. A) The driving current is set by hand and increased over time while B) the sensing voltage is logged. C) Distinct camera images, their recolored brightness distribution and their relative change in brightness with respect to picture a.

is channeled into the hottest, that is, brightest, region. At this point, the pixel experiences a rapid increase in local device temperature and brightness. Consequently, it burns-in locally. At point (c), a tristability-induced dark spot develops. The voltage then stabilizes again at an increased level (point (d)) compared to the original value at point (a). This voltage spike coincides with the spikes seen in Figure 2B.

The Switch-back effect is a necessary prerequisite for the attempted branch transition. While a tiny area of the device shows a sudden increase in temperature and current, almost all the pixel area must be in SB mode to maintain a steady total driving current. As can be seen from the relative brightness plots in Figure 3C, the shape of the SB region closely resembles the model prediction (cf., Movies S1 and S2, Supporting Information).

As can be seen from Movies S3 and S4, Supporting Information, for the 2.54 mm × 2.54 mm device, also the small pixel is in SB mode right before degradation. The crucial difference, however, is that it only gradually develops a very hot and bright region where it locally burns in. No pronounced voltage spike, which would indicate the attempted branch transition and sudden rearrangement of current and temperature distribution, can be detected here.

## 2.5. Circumventing the Distortions of Gradual Degradation

The measurement in the previous section led to the understanding of the relation between switched-back regions, tristability, and sudden device failure. The *JV* profile in Figure 2B, however, was overlaid by gradual device degradation and hence slightly deviated from the shape predicted by the simulation. In the following, we reproducibly run up and down the S-bended *IV* curve after the first burn-in event. Here, gradual degradation seems to be ceased, and the pure device behavior can now be monitored more directly (see Section S4, Supporting Information for further details).

Combining current and voltage information from measurements as presented in Figure 3, one can construct an *IV* curve that indicates the points at which the voltage has stabilized. Figure 4 presents one continuous current-stabilized *IV* measurement. For the fresh device (black squares), the voltage will not stabilize anymore at 355 mA but suddenly drop to a value at which a dark spot appears (indicated by a star) and then rise again and stabilize at a new operating point. This was discussed in Figure 3. From there, one can reproducibly scan the S-bending of the *IV* curve down (indicated by open circles) and up (solid squares). This means the OLED panel can be treated as a “new” device with new self-consistent *IVT* parameters. The same procedure can be repeated several times, each time accompanied by a reproducible voltage spike and burn-in event. The final operation characteristics (here indicated by orange open circles) can still be treated as an LED that has an elevated resistance (voltage shift to the right) with respect to the intact device. Also, with decreasing functioning area (as more and more dark spots with elevated electrical resistance arise), the S-bending is shifted upward.

While the *IV* profile of the fresh sample suffers from elevated gradual intrinsic degradation of the organic layers (almost vertical zig-zag line before break-down), the burned-in devices

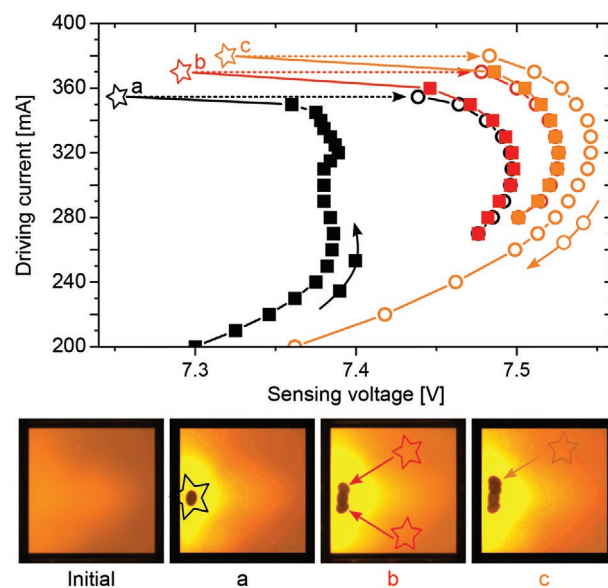


**Figure 4.** Repetitive NDR scan and branch-transition attempts. The *IV* curve is run up (solid squares) and down (open circles) several times in a row. Each burn-in is followed by an increase in voltage. After the overlaid gradual degradation in the immaculate device, the following burn-in events follow closely the predicted shape.

show very little intrinsic degradation. They are literally baked out. Their *IV* profiles follow closely the shape of the simulated curves from Figure 1A. Here, one can clearly identify that reaching the current plateau is followed by a steep voltage drop resulting in a dark spot, as was predicted by our simulation findings of tristable *IV* curves. Comparing those experimental *IV* profiles to the one from a 2.54 mm × 2.54 mm device (Movies S3 and S4, Supporting Information), the structural difference between a tristable and a bistable device characteristics becomes clearly apparent, as no current plateaus and voltage spikes are measured here. Not least, the position of the dark spots closely resembles the simulation prediction. Figure 1C suggests small spots in the left center of the device becoming too hot. This behavior is observed in the experiments by a number of different devices from several batches.

## 2.6. Saving OLEDs from Burning In

Commonly, OLEDs are driven at constant current, while voltage adjustments are required to account for gradual device degradation. With Figure 1A in mind, however, it becomes apparent that a diode can access several self-consistent operating points with dramatically deviating distributions of current and temperature. Even under gradual degradation at constant current, an OLED may switch into a different stable region while establishing thermal equilibrium (cf., Section S5, Supporting Information). An operation mode above the first stable region is hence not recommended for durable operation.

In the experiments, the transition between stable regions was seen to be not instantaneous. The voltage spike in Figure 3B could be anticipated based on the voltage adjustment features of the SMU. We were, hence, able to stop the transition from

NDR 1 into PDR 3 and save the device from irreversible burn-ins (cf., Section S6, Supporting Information). Such an intervention simply requires the differential analysis of the voltage transient. Each time a branch transition is about to happen, the voltage runaway is clearly visible in advance (cf., Figure 3B).

### 3. Conclusion

In this study, we found the *JV* curves of sufficiently large OLED lighting tiles to exhibit three stable Joule self heating-induced operating branches. This phenomenon is called tristability and has never been investigated for a thin-film device before. It causes switched-back device areas to suddenly channel a significant share of current into distinct regions of the device, thus promoting an abrupt transition into another stable operating branch. The rapid rearrangement of current distribution and temperature within the device causes local burn-in phenomena. Due to tristable behavior, neither voltage- nor current-stabilized operation modes can prevent sudden device failure, as is widely believed. Rather, the dependence of switching phenomena on the active area stresses the importance of contact technologies dividing a large lighting device effectively into smaller sub-devices.<sup>[38]</sup> It is therefore important to understand that the ratio of lateral to vertical device dimensions, as well as the interplay between the thermal conductivity parameters within the device are crucial to whether electrothermal switching does appear or not. As the Switch-back effect heralds a branch transition and the voltage transient follows a distinct profile just before device burn-in, it is possible to predict and prevent dark spot formation. Accessing the “hidden” PDR 2 region and thus proving its existence remains an interesting puzzle to be solved. Preconditioning the device in a temperature distribution which matches the one expected in PDR 2 might be one track to follow. Another possibility could be a fast switch from current-stabilized to voltage-stabilized driving mode just when the device is attempting to jump from NDR 1.

### 4. Experimental Section

**Numerical 3D Partial Differential Equation Model:** For the numerical solution of the 3D thermistor system of partial differential equations (PDE), the same code and material parameters as in ref. [23] were used. Solely the device dimensions were adapted (see Section S8, Supporting Information). The code was based on the toolbox *pdelib2*, which is developed and maintained at WIAS.<sup>[35]</sup> It was based on a Voronoi box scheme and solved a PDE system for current and heat dissipation locally for any finite element box. A short overview of the model can be found in Section S8, Supporting Information and a detailed description in ref. [34] and the references therein.

**Device Fabrication:** OLEDs were fabricated by thermal evaporation under high vacuum (Kurt J. Lesker Company) on inch-by-inch glass substrates of 1.1 mm thickness. The OLEDs have a p-i-n structure, as is commonly used, and were optimized for thermal stability. Aluminum and silver (40nm each) were used as bottom electrodes. The p-layer consisted of Spiro-TTB:C<sub>60</sub>F<sub>36</sub> (4 wt.% 40 nm), the electron-blocking layer of Spiro-TAD (10 nm), the i-layer of Spiro-TAD doped with 10 wt.% Ir(MDQ)<sub>2</sub>(acac) (20 nm), the hole-blocking layer of BaIq<sub>2</sub> (10 nm), and the n-layer of TPBi:Cs (1:1, 65 nm). On top of this stack, a transparent

top electrode was deposited (Au 2nm and Ag 7 nm). Please find the full names of the materials and *JVL* characteristics in Section S1, Supporting Information.

To prohibit air and moisture contamination, the OLED stacks were encapsulated under nitrogen atmosphere after fabrication. The encapsulation glass comprised a small cavity above the OLED pixels that prevented direct contact between sensitive materials and the encapsulation glass. It was attached to the substrate using an epoxy resin (XNR5516Z-L and XNR5590, Nagase Europa GmbH).

The device architecture was chosen for its high thermal stability and was not optimized in terms of efficiency. A luminance value of 1000 cd m<sup>-2</sup> was reached at 40 mA cm<sup>-2</sup>. The maximum EQE value was about 10.5% at 1 mA cm<sup>-2</sup>. It dropped to ≈5% at 40 mA cm<sup>-2</sup> (cf., Section S1, Supporting Information). The mean brightness shortly before degradation was estimated to reach 4500 cd m<sup>-2</sup> at current densities of 150 mA cm<sup>-2</sup>.

**Four-Wire Measurement:** Concerning the four-wire measurements, a dual-channel Keithley 2602A SMU was used to supply and measure current and voltage. The OLED was placed in a Peltier element-equipped cryostat that was controlled by a temperature controller (Belektronig, HAT control) and provided a controlled temperature that was kept at *T* = 290 K throughout the experiments. Pictures from the figures were taken by a top-mounted USB camera (Basler acA1920-40uc, Basler AG, Germany). The air pressure inside the cryostat was reduced to below 1 mbar using a pre-vacuum pumping system (Trivac D16B, Germany). Such a vacuum sufficiently rendered thermal convection insignificant in the experiments. Cryostat, temperature controller, camera, and SMU were run and controlled by the software tool SweepMe!<sup>[39]</sup> which enabled automated measurement protocols. Further information about the setup can be found in ref. [23].

### Supporting Information

Supporting Information is available from the Wiley Online Library or from the author.

### Acknowledgements

This work was supported in part by the German Research Foundation (DFG) within the Cluster of Excellence Center for Advancing Electronics Dresden (cfaed), and the DFG project HEFOS (Grant No. FI 2449/1-1) and EFOD (Grant No. RE 3198/6-1). A.G., M.L., and J.F. were partly supported by the DFG under Germany's Excellence Strategy-MATH+: The Berlin Mathematics Research Center (EXC-2046/1-project ID: 390685689) via projects AA2-10 and AA2-6. The authors thank Andreas Wendel and Tobias Günther for manufacturing the OLEDs. A.K. received funding from the Cusanuswerk Foundation.

Open access funding enabled and organized by Projekt DEAL.

### Conflict of Interest

A.F. is co-founder of “Axel Fischer und Felix Kaschura GbR” which provided the measurement software “SweepMe!” (sweep-me.net). The name of the program is given in the manuscript. The other authors declare that they have no conflict of interest.

### Data Availability Statement

The data that support the findings of this study are available from the corresponding author upon reasonable request.

## Keywords

electrothermal tristability, Joule self-heating, organic light-emitting diode lighting, sudden device burn-in

Received: July 12, 2021  
Revised: September 6, 2021  
Published online:

- 
- [1] H.-W. Chen, J.-H. Lee, B.-Y. Lin, S. Chen, S.-T. Wu, *Light: Sci. Appl.* **2018**, *7*, 17168.
- [2] L. Cao, K. Klimes, Y. Ji, T. Fleetham, J. Li, *Nat. Photonics* **2020**, *15*, 230.
- [3] P. Bobbert, R. Coehoorn, *Europhys. News* **2013**, *44*, 21.
- [4] H. Aziz, Z. D. Popovic, *Chem. Mater.* **2004**, *16*, 4522.
- [5] J. Spindler, M. Kondakova, M. Boroson, J. Hamer, V. Gohri, M. Büchel, M. Ruske, E. Meulancamp, *SID Symp. Dig. Tech. Pap.* **2016**, *47*, 294.
- [6] S. Sudheendran Swayamprabha, D. K. Dubey, R. A. K. Yadav, M. R. Nagar, A. Sharma, F.-C. Tung, J.-H. Jou, *Adv. Sci.* **2021**, *8*, 2002254.
- [7] B. Jogai, *Superlattices Microstruct.* **1992**, *11*, 383.
- [8] M. L. F. Lerch, A. D. Martin, P. E. Simmonds, L. Eaves, M. L. Leadbeater, *Solid-State Electron.* **1994**, *37*, 961.
- [9] P. D. Yoder, M. Grupen, R. K. Smith, *IEEE Trans. Electron Devices* **2010**, *57*, 3265.
- [10] M. Watanabe, H. Itoh, S. Mukai, H. Yajima, *Appl. Phys. Lett.* **1987**, *50*, 427.
- [11] S. Noda, Y. Kobayashi, T. Takayama, K. Shibata, A. Sasaki, *IEEE J. Quantum Electron.* **1992**, *28*, 2714.
- [12] Y.-C. Hsiao, K.-C. Huang, W. Lee, *Opt. Express* **2017**, *25*, 2687.
- [13] G. Krikun, K. Zojer, *J. Appl. Phys.* **2019**, *125*, 085501.
- [14] C. Kirsch, S. Altazin, R. Hiestand, T. Beierlein, R. Ferrini, T. Offermans, L. Pennick, B. Ruhstaller, *Int. J. Multiphys.* **2017**, *11*, 127.
- [15] C. Gärditz, A. Winnacker, F. Schindler, R. Paetzold, *Appl. Phys. Lett.* **2007**, *90*, 103506.
- [16] K. Neyts, M. Marescaux, A. U. Nieto, A. Elschner, W. Lövenich, K. Fehse, Q. Huang, K. Walzer, K. Leo, *J. Appl. Phys.* **2006**, *100*, 114513.
- [17] P. Schwamb, T. C. G. Reusch, C. J. Brabec, *Org. Electron.* **2013**, *14*, 1939.
- [18] K. J. Bergemann, R. Krasny, S. R. Forrest, *Org. Electron.* **2012**, *13*, 1565.
- [19] J. Ràfols-Ribé, N. D. Robinson, C. Larsen, S. Tang, M. Top, A. Sandström, L. Edman, *Adv. Funct. Mater.* **2020**, *30*, 1908649.
- [20] J. Ràfols-Ribé, E. Gracia-Espino, S. Jenatsch, P. Lundberg, A. Sandström, S. Tang, C. Larsen, L. Edman, *Adv. Opt. Mater.* **2021**, *9*, 2001405.
- [21] R. Öttking, R. Roesch, D. Fluhr, B. Muhsin, U. S. Schubert, H. Hoppe, *Sol. RRL* **2017**, *1*, 1700018.
- [22] A. Glitzky, M. Liero, G. Nika, *Discrete Contin. Dyn. Syst. - S* **2021**, *14*, 3953.
- [23] A. Kirch, A. Fischer, M. Liero, J. Fuhrmann, A. Glitzky, S. Reineke, *Light: Sci. Appl.* **2020**, *9*, 5.
- [24] A. Fischer, T. Koprucki, K. Gärtner, M. L. Tietze, J. Brückner, B. Lüssem, K. Leo, A. Glitzky, R. Scholz, *Adv. Funct. Mater.* **2014**, *24*, 3367.
- [25] A. Fischer, M. Pfalz, K. Vandewal, S. Lenk, M. Liero, A. Glitzky, S. Reineke, *Phys. Rev. Appl.* **2018**, *10*, 014023.
- [26] F. So, D. Kondakov, *Adv. Mater.* **2010**, *22*, 3762.
- [27] Z. Kohari, L. Pohl, A. Poppe, in *2012 28th Annual IEEE Semiconductor Thermal Measurement and Management Symposium (SEMI-THERM)*, IEEE, Piscataway, NJ **2012**, pp. 331–336.
- [28] Z. Kohári, E. Kollár, L. Pohl, A. Poppe, *Microelectron. J.* **2013**, *44*, 1011.
- [29] S. Y. Kim, K. Y. Kim, Y.-H. Tak, J.-L. Lee, *Appl. Phys. Lett.* **2006**, *89*, 132108.
- [30] X. Zhou, J. He, L. S. Liao, M. Lu, X. M. Ding, X. Y. Hou, X. M. Zhang, X. Q. He, S. T. Lee, *Adv. Mater.* **2000**, *12*, 265.
- [31] Z. Ding, H. Kim, D. Lee, S. Stickel, M. Boroson, J. Hamer, N. C. Giebink, *J. Appl. Phys.* **2019**, *125*, 055501.
- [32] A. Monté, J. Kundrata, J. Schram, M. Cauwe, A. Baric, J. Doutreligne, *LEUKOS* **2017**, *13*, 211.
- [33] D. K. Shin, J. W. Park, *Semicond. Sci. Technol.* **2013**, *28*, 125009.
- [34] M. Liero, J. Fuhrmann, A. Glitzky, T. Koprucki, A. Fischer, S. Reineke, *Opt. Quantum Electron.* **2017**, *49*, 330.
- [35] J. Fuhrmann, T. Streckenbach, H. Langmach, M. Uhle, WIAS-Software, <https://www.pdelib.org> (accessed: May 2021).
- [36] A. Kirch, A. Fischer, S. Reineke, M. Liero, J. Fuhrmann, A. Glitzky, *Proc. SPIE* **2020**, *11277*, 1127710.
- [37] A. Fischer, P. Pahner, B. Lüssem, K. Leo, R. Scholz, T. Koprucki, K. Gärtner, A. Glitzky, *Phys. Rev. Lett.* **2013**, *110*, 12.
- [38] G. Burwell, N. Burrige, O. J. Sandberg, E. Bond, W. Li, P. Meredith, A. Armin, *Adv. Electron. Mater.* **2020**, *6*, 2000732.
- [39] A. Fischer, F. Kaschura, SweepMe! A multi-tool measurement software, [www.sweep-me.net](http://www.sweep-me.net) (accessed: May 2021).